

Cells of a common developmental origin regulate REM/non-REM sleep and wakefulness in mice

Yu Hayashi,^{1,2*} Mitsuaki Kashiwagi,¹ Kosuke Yasuda,³ Reiko Ando,³ Mika Kanuka,¹ Kazuya Sakai,⁴ Shigeyoshi Itohara^{3*}

¹International Institute for Integrative Sleep Medicine (WPI-IIS), University of Tsukuba, 1-1-1 Tennodai Tsukuba, Ibaraki 305-8575, Japan. ²Japan Science and Technology Agency (JST), PRESTO, 4-1-8 Honcho Kawaguchi, Saitama 332-0012, Japan. ³Laboratory for Behavioral Genetics, Brain Science Institute, RIKEN, 2-1 Hirosawa, Wako-city, Saitama 351-0198, Japan. ⁴Integrative Physiology of the Brain Arousal System, Lyon Neuroscience Research Center, INSERM U1028-CNRS UMR5292, School of Medicine, Claude Bernard University Lyon 1, F-69373 Lyon, France.

*Corresponding author. E-mail: hayashi.yu.fp@u.tsukuba.ac.jp (Y.H.); sitoehara@brain.riken.jp (S.I.)

Mammalian sleep comprises rapid eye movement (REM) sleep and non-REM (NREM) sleep. To functionally isolate from the complex mixture of neurons populating the brainstem those involved in REM/NREM sleep switching, we pharmacogenetically manipulated neurons of a specific embryonic cell lineage in mice. We identified excitatory glutamatergic neurons that inhibit REM sleep and promote NREM sleep. These neurons shared a common developmental origin with neurons promoting wakefulness, both derived from a pool of proneural hindbrain cells expressing *Atoh1* at embryonic day 10.5. We also identified inhibitory GABAergic neurons that act downstream to inhibit REM sleep. Artificial reduction or prolongation of REM sleep in turn affected slow wave activity (SWA) during subsequent NREM sleep, implicating REM sleep in the regulation of NREM sleep.

Lesion and pharmacologic studies to unveil the REM/NREM sleep switch have implicated a key role for the pontine tegmentum (PT) (1–5). Within the PT, the peri-locus coeruleus (LC) α in cats and the equivalent sublaterodorsal nucleus (SLD) in rodents are critical for REM sleep induction (1, 3, 4). Neurons that negatively regulate REM sleep or promote the exit from REM sleep are far less understood, however, and whether such neurons locate within the PT is unclear. Various models have proposed the importance of interactions between cholinergic, monoaminergic, GABAergic, and glutamatergic neurons for sleep stage switching (2, 4, 5). Except for the glutamatergic nature of REM sleep-promoting neurons in the SLD (6), the molecular identity and precise location of neurons participating in REM/NREM sleep switching remain elusive.

We focused on the embryonic cell lineage as a feature to isolate neurons with a specific function in sleep. The cerebellar rhombic lip (CRL), a neuroepithelial structure that emerges transiently in the vertebrate embryo, is the major source of cerebellar granule cells (7), but a subset of cells originating between embryonic days [E] 10–12 migrate to the rostral hindbrain and contribute to a subpopulation of excitatory neurons in the PT (8–10). These cells transiently express the proneural transcription factor gene *Atoh1*

(*Atonal homolog 1*, *Math1*) (8, 9), and can be precisely genetically labeled using the *Atoh1* enhancer (8, 11). We developed a transgenic mouse expressing the tamoxifen-inducible form of Cre (CreER^{T2}) under the *Atoh1* enhancer (*Atoh1-CreER^{T2}*). Crossing these mice with a Cre-dependent *Rosa26-loxP-stop-loxP(LSL)-NLS-lacZ* reporter strain (12) and administering tamoxifen at E10.5 resulted in reporter expression in cells migrating from the CRL at E13.5 (fig. S1A) and dispersedly distributing within the PT in adult mice (fig. S1, B to D) (8). These neurons (*Atoh1*-E10.5 cells) were either glutamatergic or cholinergic, based on the expression of *vesicular glutamate transporter 2* (*Vglut2*) or choline acetyltransferase (ChAT), respectively, but not GABAergic or noradrenergic, based on the expression of *glutamate decarboxylase 1* or tyrosine hydroxylase, respectively (fig. S1, E to H). These PT neurons did not derive from rhombic lip areas caudal to the CRL, as they were included

in the midbrain-rhombomere1 derived domain, which can be labeled using *En1-Cre* (8, 13) (fig. S1I).

We first tested the effect of activating the *Atoh1*-E10.5 cells with DREADD (designer receptors exclusively activated by designer drugs) technology (14). *Atoh1-CreER^{T2}* mice were crossed with transgenic mice carrying a Cre-dependent tetracycline transactivator (tTA) transgene (*CAG-LSL-tTA*) (15) and administered tamoxifen at E10.5. Postnatally, we microinjected a recombinant adenoassociated virus (AAV) carrying a tTA-dependent hM3Dq transgene (AAV-TRE-hM3Dq-mCherry) (Fig. 1A) targeting two *Atoh1*-E10.5 subpopulations (Figs. 1, 2): *Atoh1*-E10.5-medial cells, located ventromedial to the medial part of the superior cerebellar peduncle (scp) between the ventral part of the laterodorsal tegmentum (LDTgV) and the medial parabrachial nucleus (MPB) (fig. S1D and Fig. 1, A and B); and *Atoh1*-E10.5-lateral cells, located dorsolateral to the scp within the lateral parabrachial nucleus (LPB) (fig. S1D and Fig. 2, A and B). hM3Dq is a DREADD receptor that evokes neural excitation upon binding of its ligand, clozapine-N-oxide (CNO). In both brain areas, CNO administration efficiently induced c-Fos expression, a marker of neural excitation (fig. S2).

We next evaluated the effect of exciting *Atoh1*-E10.5-medial cells (Fig. 1 and fig. S3). CNO was administered to

three groups: mice double-transgenic for *CreER^{T2}* and *tTA* and transfected with *hM3Dq*-carrying AAV (dTg + *hM3Dq*) or with green fluorescent protein (*GFP*)-carrying AAV (dTg + *GFP*) to control for any non-specific effects of CNO, and mice solely transgenic for *tTA* and transfected with *hM3Dq*-carrying AAV (sTg + *hM3Dq*) to control for any Cre non-dependent expression of *hM3Dq*. When *Atoh1*-E10.5-medial cells were excited during the light phase (zeitgeber time [ZT] 5), REM sleep was drastically reduced and NREM sleep was increased in a Cre- and *hM3Dq*-dependent manner (Fig. 1C and fig. S3A). The large reduction in the REM sleep amount was due to a decrease in both the number and duration of REM sleep episodes, implying that these neurons regulate both entry into and exit from REM sleep (fig. S3, B and C). Unilateral injection of AAV was sufficient for these effects. Applying CNO during the dark phase produced similar effects (ZT 15) (fig. S3D). Awake periods appeared unaffected, suggesting that these neurons regulate REM/NREM sleep switching, but not sleep/wake switching.

Electroencephalography (EEG) properties during sleep vary among cortical areas (16). Simultaneously recording EEG from the frontal and parietal cortices showed that transitions from NREM sleep to REM sleep are asynchronous between the two cortical areas (fig. S4A) (16). This asynchronous state (termed transitory state) was reduced in the experimental group, indicating that the reduced REM sleep was not due to an extension of the transitory state (fig. S4, B to E).

Atoh1-E10.5 cells are either glutamatergic or cholinergic. To determine which subtype regulates REM/NREM sleep, we used the *Camk2a-LSL-tTA* strain (17). This largely reduced AAV transgene expression in cholinergic neurons (fig. S5), and yet CNO administration efficiently reduced REM sleep (fig. S3, E to G). We generated a transgenic mouse in which *tTA* expression was Cre-dependent and under the control of the glutamatergic neuron-specific gene *Vglut2* promoter (*Vglut2-LSL-tTA*). This also reduced cholinergic neurons expressing the AAV transgene (fig. S5), and still CNO administration efficiently reduced REM sleep (fig. S3, H to J). These findings strongly suggest that, of the *Atoh1*-E10.5-medial cells, glutamatergic neurons regulate REM/NREM sleep. These neurons locate near the REM sleep-promoting neurons in the SLD, but are more rostro-lateral (4, 6).

We then tested the effect of activating *Atoh1*-E10.5-lateral cells (Fig. 2 and fig. S6). Animals spent more time awake at the expense of both REM and NREM sleep (Fig. 2C and fig. S6A). Sleep was highly fragmented, resulting in increased numbers of both awake and NREM sleep episodes (fig. S6B). The *Atoh1*-E10.5-lateral cells that promote wakefulness are also likely glutamatergic, because the use of *Camk2a-LSL-tTA* had similar effects (fig. S6, D to F). These *Atoh1*-E10.5-lateral cells likely overlap with previously reported awake-promoting glutamatergic neurons in the lateral parabrachial nucleus (18). A correlation analysis of the AAV transfection

range and effect on NREM sleep amount demonstrated distinct roles of *Atoh1*-E10.5-lateral cells and -medial cells in sleep regulation (Fig. 2D).

Atoh1-E10.5-medial cells are glutamatergic neurons that promote NREM sleep and inhibit REM sleep. We examined possible targets of these neurons by expressing GFP and tracking their axons (Fig. 3A). Axons were detected in areas rostral to but not caudal to the soma. Axonal varicosities, reminiscent of presynaptic structures, were detected bilaterally within the midbrain, in the dorsal area of the deep mesencephalic nucleus (dDpMe) (Fig. 3, B and C). The dDpMe and adjacent ventrolateral periaqueductal grey matter (vlPAG) contain neurons that negatively regulate REM sleep, although the type of neuron responsible is unknown (4, 19, 20). We examined the roles of inhibitory neurons, because they send axons to the SLD (21). AAV carrying Cre-dependent transgenes were bilaterally microinjected into this area in a knockin (KI) mouse strain expressing Cre under control of the *vesicular GABA transporter (Vgat)* promoter (*Vgat-Cre* KI) (22) (Fig. 3D). Cre-derived transgene expression was detected almost exclusively in GABAergic neurons, as assessed by coexpression with *glutamate decarboxylase 1* (fig. S7A). Axonal varicosities of these GABAergic neurons were detected in the dorsocaudal area of the PT, which includes the SLD (Fig. 3E). CNO administration induced c-Fos expression in these neurons when *hM3Dq* was expressed (fig. S7, B to D). Similar to *Atoh1*-E10.5-medial cells, stimulating dDpMe inhibitory neurons at ZT 5 or ZT 15 reduced REM sleep and increased NREM sleep (Fig. 3F and fig. S8, A, C, E, and G). By contrast, *hM4Di* expression, a DREADD receptor that inhibits neural excitation upon binding of CNO, increased REM sleep, mainly by increasing REM sleep episode numbers (Fig. 3G and fig. S8, H, J, and L). Similar results were observed in a transgenic mouse strain carrying *Vgat-Cre (Vgat-Cre Tg)* (23) (fig. S8, B, D, F, I, K, and M). Thus, dDpMe inhibitory neurons negatively regulate REM sleep, possibly by inhibiting REM-promoting neurons in the SLD. *Atoh1*-E10.5-medial cells might help to regulate REM/NREM sleep switching by activating these neurons. dDpMe neurons fire maximally during REM sleep, increasing their firing rate toward the end of REM sleep episodes (19). Thus, it might be that, during REM sleep, a gradual increase in dDpMe neuron firing promotes the exit from REM sleep, whereas basal activity during NREM sleep regulates entry into REM sleep, although further studies with cell-type specificity are required.

REM sleep is homeostatically regulated, and REM sleep deprivation (REMD) leads to a subsequent rebound (24). We examined the effect of 6-hours REMD from ZT 0 to ZT 6 on REM sleep inhibition caused by activating dDpMe inhibitory neurons (fig. S9). During REMD, REM sleep amount was reduced from 6~7% to less than 0.8% (fig. S9, B to D), and the number of entries into REM sleep gradually increased (fig. S9E), suggesting an increased REM sleep pressure. Even under increased REM sleep pressure following REMD,

dDpMe inhibitory neurons strongly suppressed REM sleep (fig. S9, F and G). Thus, negative regulation of these neurons might underlie the homeostatic REM sleep rebound, or artificial activation of these neurons might erase (or override) the preceding history of REM sleep loss.

The function of REM sleep is poorly understood. Longer REM sleep episodes are associated with longer subsequent NREM sleep episodes, suggesting that REM sleep contributes to NREM sleep expression (25). We assessed this hypothesis using our transgenic systems to manipulate REM sleep. We first examined whether REM sleep enhances SWA during subsequent NREM sleep, as higher SWA is associated with longer NREM sleep episodes. SWA, typically quantified as the spectral power of EEG in the delta range (0.5-4 Hz), reflects synchronized oscillations of cortical membrane potential and is most prominent during deep NREM sleep. Moreover, SWA contributes to synaptic plasticity and memory consolidation (26, 27). We analyzed the correlation between naturally occurring REM sleep episode duration and delta power in the subsequent NREM sleep. Absolute delta power was not compared because it is highly variable, even within the same individual (28). Therefore, the mean delta power of the subsequent NREM sleep episode (NREM_b) was calculated relative to the previous NREM sleep episode (NREM_a; fig. S10A; see Supplementary Methods for details), which revealed a significant positive correlation (fig. S10B). A previous study in humans did not reveal a significant correlation (29). This might be because absolute delta power was used for the previous analyses, which did not show a significant correlation in our study either, although a difference between mouse and human is also possible.

To determine whether REM sleep occurrence led to NREM sleep SWA enhancement, we manipulated REM sleep by pharmacogenetically activating or inhibiting the identified sleep regulatory circuit. First, REM sleep was transiently reduced by DREADD-activation of either *Atoh1-E10.5* medial cells or dDpMe inhibitory neurons. During reduced REM sleep, the NREM sleep delta power gradually decreased (Fig. 4, A and B). SWA seemed to recover immediately following REM sleep recovery (Fig. 4B, fig. S11). We defined three classes of REM sleep episodes: natural REM, shortened REM, and post-DREADD REM (fig. S12; see Supplementary Materials for details). We compared the EEG spectra of these episodes as well as the NREM, transitory, or awake episodes surrounding them (fig. S13). Shortened REM was associated with a slight increase in the delta range power (fig. S13A). By contrast, NREM sleep episodes around shortened REM initially appeared unaffected, whereas delta power was reduced after prolonged REM sleep inhibition (fig. S13C). The reduction in delta power recovered in the NREM episode immediately following post-DREADD REM (fig. S13C).

Next, in each class of REM sleep, we compared the mean normalized delta power between NREM_a and NREM_b.

SWA in NREM_b following shortened REM was reduced compared to NREM_a, whereas SWA in NREM_b following post-DREADD REM was increased (Fig. 4, C to E). In addition, DREADD-inhibition of dDpMe inhibitory neurons occasionally evoked long REM sleep episodes of at least 4 min, which were never observed under other conditions, although the mean REM sleep episode duration was not significantly changed (fig. S8, L and M). These REM sleep episodes, which we termed “prolonged REM”, were followed by NREM_b with increased SWA (Fig. 4F). Our results are somewhat consistent with a study in humans showing that SWA during NREM sleep is gradually reduced during selective REM sleep deprivation and returns to the initial level following REM sleep recovery (30), although we cannot completely exclude the involvement of a third factor evoked by the DREADD manipulation (e.g. hormone levels, neurotransmitters, etc.).

During the late light phase, when all SWA data were collected, NREM sleep episodes were occasionally interrupted by short awake episodes. These NREM-intervening awake episodes were followed by NREM_b with significantly reduced delta power (Fig. 4G). Thus, in contrast to the well-known SWA-enhancing effect of long awake periods lasting several hours (31), the NREM-intervening episodes observed here, which did not exceed ~13 min, did not increase SWA. We plotted the relative delta power of NREM_b against the episode duration of REM sleep episodes or NREM-intervening awake episodes (Fig. 4, H and I). While delta power was significantly and positively correlated with REM sleep episode duration, no obvious correlation with NREM-intervening wakefulness was observed. Similar results were obtained when we separately plotted results from mice harboring *Atoh1-CreER^{T2}* or *Vgat-Cre* (fig. S14). A unique cortical activity or neuromodulator release mode during REM sleep might underlie the strong enhancement of SWA during ensuing NREM sleep. As SWA is most intense in the first NREM sleep cycle in humans, and sleep deprivation also enhances subsequent SWA, homeostatic NREM sleep pressure accumulating during the awake state is likely the major factor for SWA enhancement. Our findings therefore suggest another role for REM sleep. Finally, our transgenic system for REM sleep inhibition might also be effective for testing other proposed REM sleep functions, including brain development (32) and memory processing.

Our developmental cell fate mapping approach allowed us to identify a single genetically marked cell population that contributes to two distinct aspects of sleep regulation: neurons that promote NREM sleep at the expense of REM sleep, and neurons that promote wakefulness at the expense of sleep. The awake and NREM sleep states differ in terms of the level of consciousness, but share other features such as the presence of muscle tone and integrated thermoregulatory responses or respiration. Direct transitions from wakefulness to REM sleep do not occur in healthy states. Thus, REM sleep-promoting neurons are likely strongly in-

hibited during wakefulness. Both *Atoh1*-E10.5-medial and -lateral cells might share a common feature to inhibit the REM-promoting system, although cortical activating functions in lateral cells might be substituted for by a cortical synchronizing function in the medial cells. During evolution, REM/NREM sleep stages might have emerged from the modification of a subset of cells regulating sleep/wake cycles. The abundance of REM sleep in neonates (32) and the confinement of increased SWA during NREM sleep in birds and mammals suggest that REM sleep closely resembles prototype sleep in ancestral animals. Further investigations of the function of *Atoh1*-E10.5 cell equivalents in animals lacking obvious REM/NREM sleep, such as reptiles, might be meaningful toward understanding the evolution of mammalian sleep to its current complex state. In summary, our cell lineage tracing approach in combination with pharmacogenetic tools will be useful for further investigation of the evolutionary origin and function of sleep, and other circuits controlling complex behaviors.

REFERENCES AND NOTES

- G. Vanni-Mercier, K. Sakai, J. S. Lin, M. Jouvet, Mapping of cholinergic brainstem structures responsible for the generation of paradoxical sleep in the cat. *Arch. Ital. Biol.* **127**, 133–164 (1989). [Medline](#)
- K. Sakai, S. Crochet, H. Onoe, Pontine structures and mechanisms involved in the generation of paradoxical (REM) sleep. *Arch. Ital. Biol.* **139**, 93–107 (2001). [Medline](#)
- R. Boissard, D. Gervasoni, M. H. Schmidt, B. Barbagli, P. Fort, P. H. Luppi, The rat ponto-medullary network responsible for paradoxical sleep onset and maintenance: A combined microinjection and functional neuroanatomical study. *Eur. J. Neurosci.* **16**, 1959–1973 (2002). [Medline](#) [doi:10.1046/j.1460-9568.2002.02257.x](#)
- J. Lu, D. Sherman, M. Devor, C. B. Saper, A putative flip-flop switch for control of REM sleep. *Nature* **441**, 589–594 (2006). [Medline](#) [doi:10.1038/nature04767](#)
- P. H. Luppi, O. Clement, E. Sapin, C. Peyron, D. Gervasoni, L. Léger, P. Fort, Brainstem mechanisms of paradoxical (REM) sleep generation. *Pflügers Arch.* **463**, 43–52 (2012). [Medline](#) [doi:10.1007/s00424-011-1054-y](#)
- M. Krenzer, C. Anaclet, R. Vetrivelan, N. Wang, L. Vong, B. B. Lowell, P. M. Fuller, J. Lu, Brainstem and spinal cord circuitry regulating REM sleep and muscle atonia. *PLOS ONE* **6**, e24998 (2011). [Medline](#)
- J. Alder, N. K. Cho, M. E. Hatten, Embryonic precursor cells from the rhombic lip are specified to a cerebellar granule neuron identity. *Neuron* **17**, 389–399 (1996). [Medline](#) [doi:10.1016/S0896-6273\(00\)80172-5](#)
- R. Machold, G. Fishell, Math1 is expressed in temporally discrete pools of cerebellar rhombic-lip neural progenitors. *Neuron* **48**, 17–24 (2005). [Medline](#) [doi:10.1016/j.neuron.2005.08.028](#)
- V. Y. Wang, M. F. Rose, H. Y. Zoghbi, Math1 expression redefines the rhombic lip derivatives and reveals novel lineages within the brainstem and cerebellum. *Neuron* **48**, 31–43 (2005). [Medline](#) [doi:10.1016/j.neuron.2005.08.024](#)
- M. J. Green, A. M. Myat, B. A. Emmenegger, R. J. Wechsler-Reya, L. J. Wilson, R. J. Wingate, Independently specified *Atoh1* domains define novel developmental compartments in rhombomere 1. *Development* **141**, 389–398 (2014). [Medline](#) [doi:10.1242/dev.099119](#)
- A. W. Helms, A. L. Abney, N. Ben-Arie, H. Y. Zoghbi, J. E. Johnson, Autoregulation and multiple enhancers control Math1 expression in the developing nervous system. *Development* **127**, 1185–1196 (2000). [Medline](#)
- Y. Kobayashi, Y. Sano, E. Vannoni, H. Goto, H. Suzuki, A. Oba, H. Kawasaki, S. Kanba, H. P. Lipp, N. P. Murphy, D. P. Wolfer, S. Itohara, Genetic dissection of medial habenula-interpeduncular nucleus pathway function in mice. *Front. Behav. Neurosci.* **7**, 17 (2013). [Medline](#) [doi:10.3389/fnbeh.2013.00017](#)
- M. Zervas, S. Millet, S. Ahn, A. L. Joyner, Cell behaviors and genetic lineages of the mesencephalon and rhombomere 1. *Neuron* **43**, 345–357 (2004). [Medline](#) [doi:10.1016/j.neuron.2004.07.010](#)
- B. N. Armbruster, X. Li, M. H. Pausch, S. Herlitze, B. L. Roth, Evolving the lock to fit the key to create a family of G protein-coupled receptors potentially activated by an inert ligand. *Proc. Natl. Acad. Sci. U.S.A.* **104**, 5163–5168 (2007). [Medline](#) [doi:10.1073/pnas.0700293104](#)
- K. Miyamichi, F. Amat, F. Moussavi, C. Wang, I. Wickersham, N. R. Wall, H. Taniguchi, B. Tasic, Z. J. Huang, Z. He, E. M. Callaway, M. A. Horowitz, L. Luo, Cortical representations of olfactory input by trans-synaptic tracing. *Nature* **472**, 191–196 (2011). [Medline](#) [doi:10.1038/nature09714](#)
- V. V. Vyazovskiy, P. Achermann, A. A. Borbély, I. Tobler, The dynamics of spindles and EEG slow-wave activity in NREM sleep in mice. *Arch. Ital. Biol.* **142**, 511–523 (2004). [Medline](#)
- T. Nakashiba, J. Z. Young, T. J. McHugh, D. L. Buhl, S. Tonegawa, Transgenic inhibition of synaptic transmission reveals role of CA3 output in hippocampal learning. *Science* **319**, 1260–1264 (2008). [Medline](#) [doi:10.1126/science.1151120](#)
- S. Kaur, N. P. Pedersen, S. Yokota, E. E. Hur, P. M. Fuller, M. Lazarus, N. L. Chamberlin, C. B. Saper, Glutamatergic signaling from the parabrachial nucleus plays a critical role in hypercapnic arousal. *J. Neurosci.* **33**, 7627–7640 (2013). [Medline](#) [doi:10.1523/JNEUROSCI.0173-13.2013](#)
- S. Crochet, H. Onoe, K. Sakai, A potent non-monoaminergic paradoxical sleep inhibitory system: A reverse microdialysis and single-unit recording study. *Eur. J. Neurosci.* **24**, 1404–1412 (2006). [Medline](#) [doi:10.1111/j.1460-9568.2006.04995.x](#)
- E. Sapin, D. Lapray, A. Bérod, R. Goutagny, L. Léger, P. Ravassard, O. Clément, L. Hanriot, P. Fort, P. H. Luppi, Localization of the brainstem GABAergic neurons controlling paradoxical (REM) sleep. *PLOS ONE* **4**, e4272 (2009). [Medline](#) [doi:10.1371/journal.pone.0004272](#)
- R. Boissard, P. Fort, D. Gervasoni, B. Barbagli, P. H. Luppi, Localization of the GABAergic and non-GABAergic neurons projecting to the sublaterodorsal nucleus and potentially gating paradoxical sleep onset. *Eur. J. Neurosci.* **18**, 1627–1639 (2003). [Medline](#) [doi:10.1046/j.1460-9568.2003.02861.x](#)
- L. Vong, C. Ye, Z. Yang, B. Choi, S. Chua Jr., B. B. Lowell, Leptin action on GABAergic neurons prevents obesity and reduces inhibitory tone to POMC neurons. *Neuron* **71**, 142–154 (2011). [Medline](#) [doi:10.1016/j.neuron.2011.05.028](#)
- I. Ogiwara, T. Iwasato, H. Miyamoto, R. Iwata, T. Yamagata, E. Mazaki, Y. Yanagawa, N. Tamamaki, T. K. Hensch, S. Itohara, K. Yamakawa, Nav1.1 haploinsufficiency in excitatory neurons ameliorates seizure-associated sudden death in a mouse model of Dravet syndrome. *Hum. Mol. Genet.* **22**, 4784–4804 (2013). [Medline](#) [doi:10.1093/hmg/ddt331](#)
- T. Endo, B. Schwierin, A. A. Borbély, I. Tobler, Selective and total sleep deprivation: Effect on the sleep EEG in the rat. *Psychiatry Res.* **66**, 97–110 (1997). [Medline](#) [doi:10.1016/S0165-1781\(96\)03029-6](#)
- J. H. Benington, H. C. Heller, Does the function of REM sleep concern non-REM sleep or waking? *Prog. Neurobiol.* **44**, 433–449 (1994). [Medline](#) [doi:10.1016/0301-0082\(94\)90005-1](#)
- L. Marshall, H. Helgadóttir, M. Mölle, J. Born, Boosting slow oscillations during sleep potentiates memory. *Nature* **444**, 610–613 (2006). [Medline](#) [doi:10.1038/nature05278](#)
- S. Chauvette, J. Seigneur, I. Timofeev, Sleep oscillations in the thalamocortical system induce long-term neuronal plasticity. *Neuron* **75**, 1105–1113 (2012). [Medline](#) [doi:10.1016/j.neuron.2012.08.034](#)
- V. V. Vyazovskiy, B. A. Riedner, C. Cirelli, G. Tononi, Sleep homeostasis and cortical synchronization: II. A local field potential study of sleep slow waves in the rat. *Sleep* **30**, 1631–1642 (2007). [Medline](#)
- O. Le Bon, P. Linkowski, Absence of systematic relationships between REMS duration episodes and spectral power Delta and Ultra-Slow bands in contiguous NREMS episodes in healthy humans. *J. Neurophysiol.* **110**, 162–169 (2013). [Medline](#) [doi:10.1152/jn.00020.2013](#)
- D. G. Beersma, D. J. Dijk, C. G. Blok, I. Everhardus, REM sleep deprivation during 5 hours leads to an immediate REM sleep rebound and to suppression of non-REM sleep intensity. *Electroencephalogr. Clin. Neurophysiol.* **76**, 114–122 (1990). [Medline](#) [doi:10.1016/0013-4694\(90\)90209-3](#)
- A. Suzuki, C. M. Sinton, R. W. Greene, M. Yanagisawa, Behavioral and biochemical dissociation of arousal and homeostatic sleep need influenced by prior wakeful experience in mice. *Proc. Natl. Acad. Sci. U.S.A.* **110**, 10288–10293 (2013). [Medline](#) [doi:10.1073/pnas.1308295110](#)
- H. P. Roffwarg, J. N. Muzio, W. C. Dement, Ontogenetic development of the human sleep-dream cycle. *Science* **152**, 604–619 (1966). [Medline](#) [doi:10.1126/science.152.3722.604](#)
- L. Madisen, T. A. Zwingman, S. M. Sunkin, S. W. Oh, H. A. Zariwala, H. Gu, L. L. Ng,

R. D. Palmiter, M. J. Hawrylycz, A. R. Jones, E. S. Lein, H. Zeng, A robust and high-throughput Cre reporting and characterization system for the whole mouse brain. *Nat. Neurosci.* **13**, 133–140 (2010). [Medline doi:10.1038/nn.2467](https://doi.org/10.1038/nn.2467)

ACKNOWLEDGMENTS

We thank M. Yanagisawa for support of experiments and critical reading of the manuscript; H. Hirase, Y. Koyama, and M. Matsumata for technical advice; C. Yokoyama and S. Tonegawa for comments on the manuscript; L. Luo, S. Tonegawa, T. Kaneko, B. Roth, C. Cepko, and K. Deisseroth for providing reagents; and all members of the Itohara laboratory and Hayashi laboratory for their support and discussion. CAG-LSL-tTA and Camk2-LSL-tTA mice were provided under a materials transfer agreement with Stanford Univ. and MIT, respectively. This work was supported by the JST PRESTO program, the MEXT World Premier International Research Center Initiative (WPI), the MEXT KAKENHI for Scientific Research on Innovative Areas "Systems Molecular Ethology" (23115724) and "Memory Dynamism" (26115503), JSPS KAKENHI Grant Numbers 23700403 and 21800090, the Mochida Memorial Foundation for Medical and Pharmaceutical Research, the Astellas Foundation for Research on Metabolic Disorders, the Sumitomo Foundation Grant for Basic Science Research Projects, the SENSHIN Medical Research Foundation, the Japan Foundation for Applied Enzymology (TMFC), and the RIKEN Special Postdoctoral Researcher Program (to Y.H.), and the Funding Program for World-Leading Innovative R&D on Science and Technology (FIRST Program) initiated by the Council for Science and Technology Policy (CSTP) and the RIKEN intramural fund (to S.I.). All data are stored in the International Institute for Integrative Sleep Medicine, University of Tsukuba and the Brain Science Institute, RIKEN.

SUPPLEMENTARY MATERIALS

www.sciencemag.org/cgi/content/full/science.aad1023/DC1

Materials and Methods
Supplementary Text
Figs. S1 to S14
Reference (33)
Data file S1

27 July 2015; accepted 7 October 2015

Published online 22 October 2015

10.1126/science.aad1023

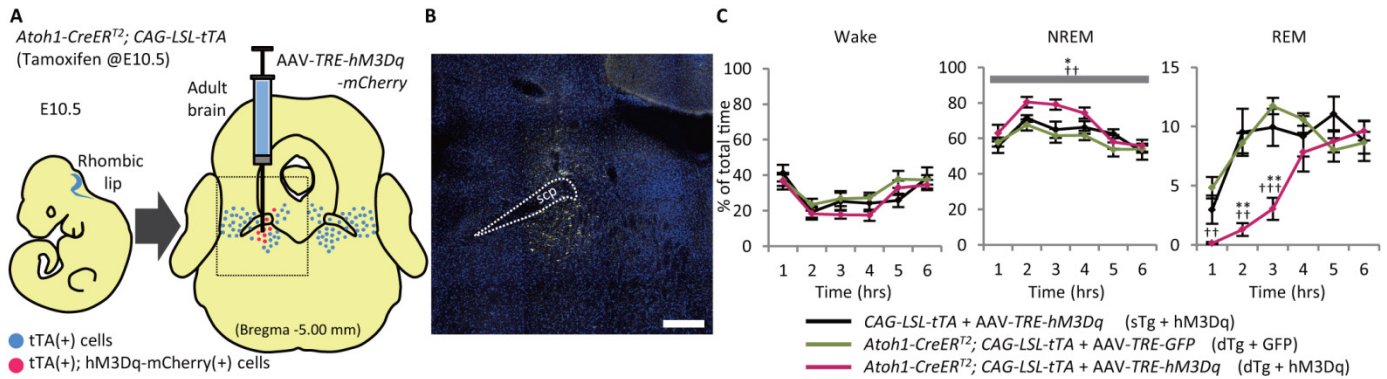


Fig. 1. *Atoh1*-E10.5-medial cells regulate REM/NREM sleep. (A) Labeling of *Atoh1*-E10.5 cells with tTA (left) and injection of AAV carrying tTA-dependent *hM3Dq-mCherry* into an area medioventral to the scp, between LDTgV and MPB (right). (B) *hM3Dq-mCherry* expression (yellow) in a region corresponding to the enclosed area in (A). Counterstain: DAPI (blue). Scale bar, 200 μ m. (C) Pharmacogenetic activation of neurons in (B) increased NREM sleep and reduced REM sleep, but had no significant effect on wakefulness. Horizontal axes indicate time after CNO administration. Data represent mean \pm s.e.m. $n = 8$ animals/group. *, $\dagger p < 0.05$, **, $\dagger\dagger p < 0.005$, ***, $\dagger\dagger\dagger p < 0.001$ (post-hoc Tukey HSD test, *: dTg + hM3Dq VS sTg + hM3Dq, \dagger : dTg + hM3Dq VS dTg + GFP).

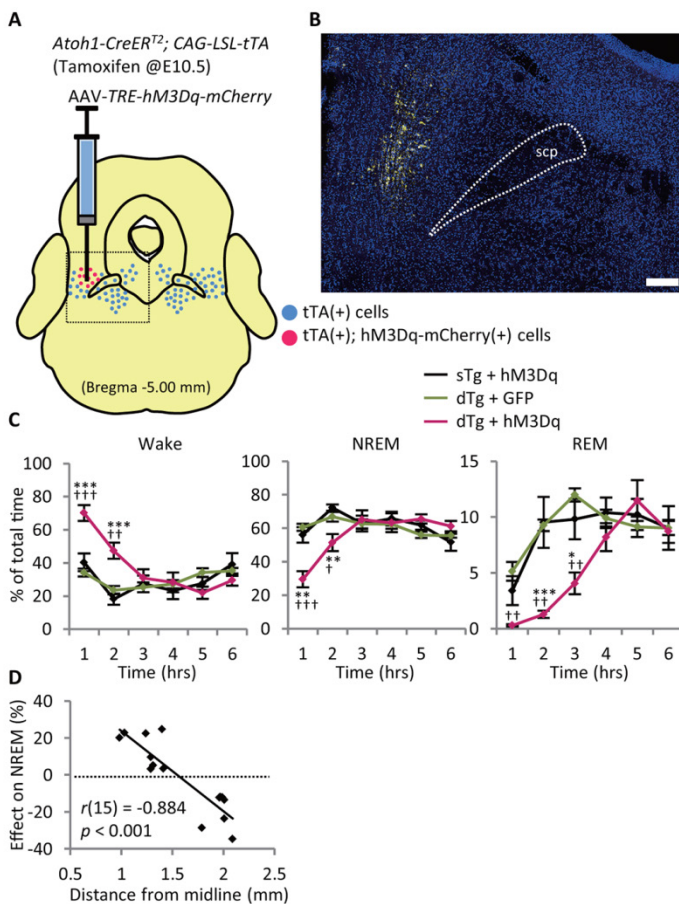


Fig. 2. *Atoh1*-E10.5-lateral cells regulate sleep/wake ratio. (A) Injection of AAV carrying tTA-dependent *hM3Dq-mCherry* dorsolateral to the scp, within the LPB. (B) *hM3Dq-mCherry* expression (yellow) in a region corresponding to the enclosed area in (A). Counterstain: DAPI (blue). Scale bar, 200 μ m. (C) Pharmacogenetic activation of neurons in (B) increased awake state and reduced NREM sleep and REM sleep. Horizontal axes indicate time after CNO administration. Data represent mean \pm s.e.m. $n = 7$ animals/group. *, $\dagger p < 0.05$, **, $\dagger\dagger p < 0.005$, ***, $\dagger\dagger\dagger p < 0.001$ (post-hoc Tukey HSD test, *: dTg + hM3Dq VS sTg + hM3Dq, \dagger : dTg + hM3Dq VS dTg + GFP). (D) Correlation between location of *hM3Dq*-expressing cell medial boundary and effect on NREM sleep. Each dot represents an individual mouse (dTg + hM3Dq), and the vertical axis indicates NREM sleep amount at 2 hours after CNO administration relative to that after saline administration. Pearson correlation coefficient r and level of significance p in two-tailed test are indicated.

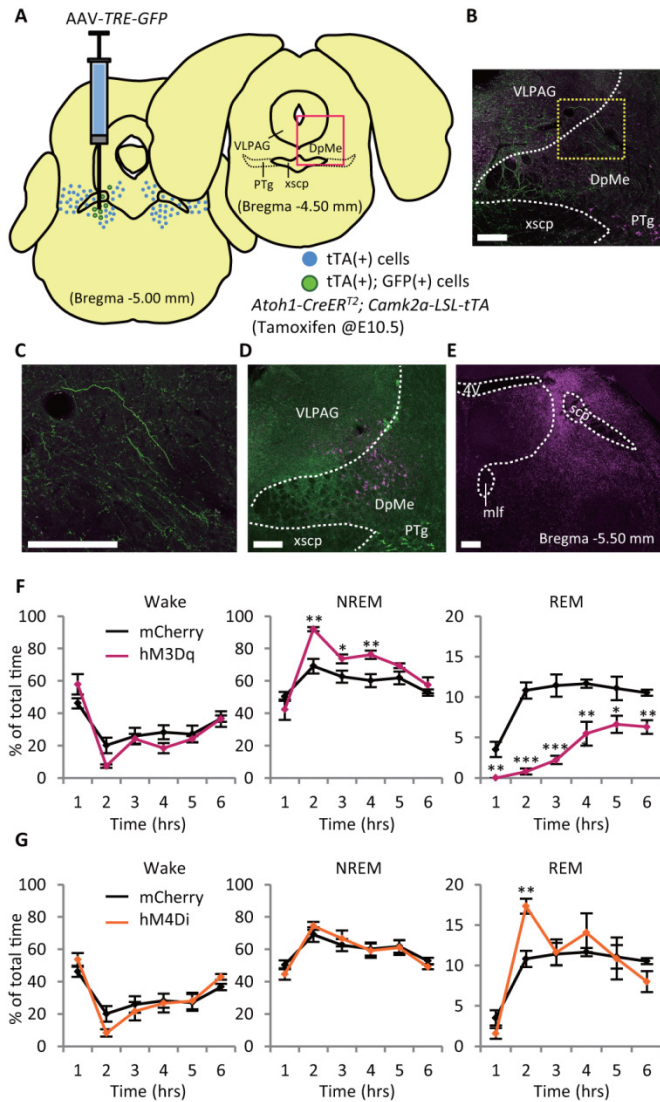


Fig. 3. Inhibitory neurons in dDpMe inhibit REM sleep. (A) Injection of AAV carrying tTA-dependent GFP into an area ventromedial to the scp (same area as Fig. 1A). xscp, decussation of the superior cerebellar peduncle. (B) GFP (green)-positive axons were detected in a region rostral and contralateral to the AAV injection site, corresponding to the enclosed area in (A). Counterstain: ChAT (magenta). (C) Higher magnification of the area enclosed in (B). GFP-positive axon varicosities were detected. (D) AAV carrying Cre-dependent hM4Di-mCherry (magenta) was injected into dDpMe of *Vgat-Cre* KI mice. Counterstain: ChAT (green). (E) hM4Di-mCherry (magenta)-positive axon varicosities were detected in a wide area in the dorso-caudal region of the pontine tegmentum. 4V, fourth ventricle. mlf, medial longitudinal fasciculus. (F and G) Pharmacogenetic activation (F) or inhibition (G) of dDpMe inhibitory neurons reduced or increased REM sleep, respectively. Horizontal axes indicate time after CNO administration. Data represent mean \pm s.e.m. $n = 6$ animals/group. * $p < 0.05$, ** $p < 0.005$, *** $p < 0.001$ (one-way ANOVA). Scale bars, 200 μ m.

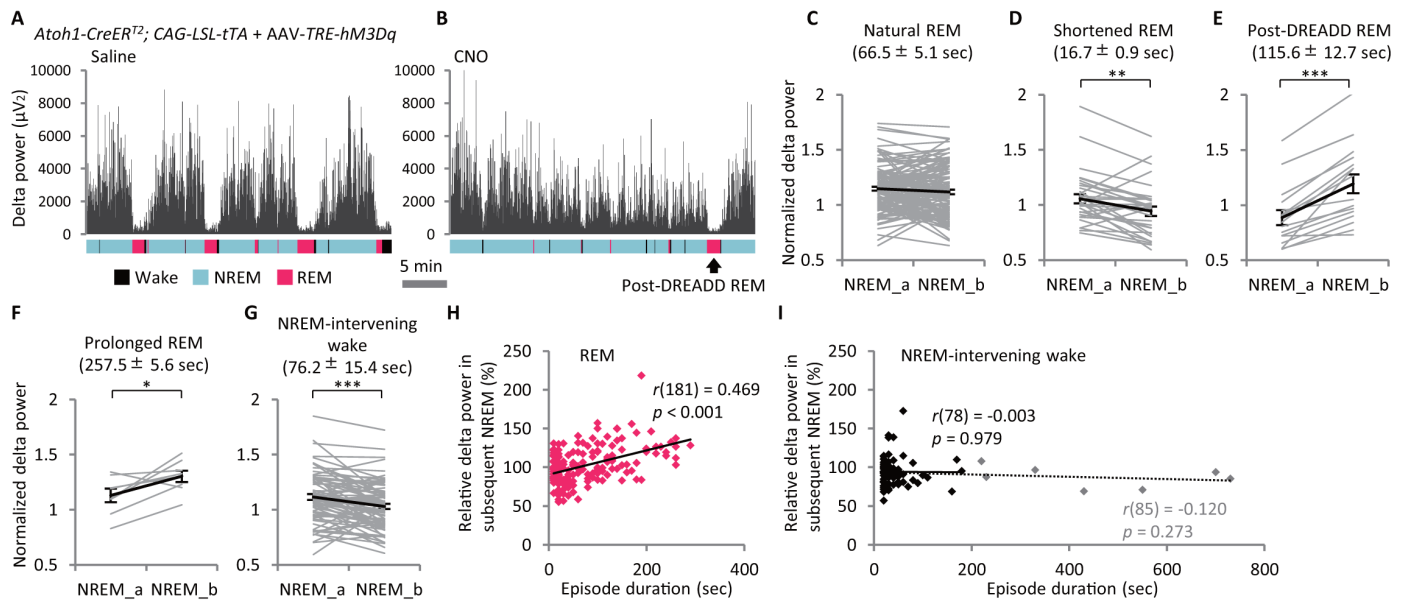


Fig. 4. REM sleep inhibition or extension affects SWA in subsequent NREM sleep. (A and B) Examples of delta power change after administering saline (A) or CNO (B) to a mouse expressing hM3Dq in REM sleep-inhibiting neurons. (C to G) Comparison of mean relative delta power in NREM sleep episodes prior to (NREM_a) and immediately after (NREM_b) indicated REM sleep or awake episode. “Shortened REM” refers to REM sleep episodes less than 50% the mean duration that appeared following CNO administration. “Post-DREADD REM” refers to the first REM sleep episode following “shortened REM”. “Natural REM” refers to REM sleep episodes in mice transfected with control AAV and administered CNO. See Supplementary Materials and fig. S12 for details. Numbers in parentheses indicate mean episode duration \pm s.e.m. Grey lines represent pairs of NREM sleep episodes. Black lines represent mean \pm s.e.m. * $p < 0.05$, ** $p < 0.005$, *** $p < 0.001$ (within-within-subjects ANOVA). (H and I) Correlation between NREM_b to NREM_a ratio and duration of intervening REM sleep (H) or intervening awake (I) episode. Pearson correlation coefficient r and level of significance p in two-tailed test are indicated. Statistical outliers and analyses including the outliers are indicated in grey.